ACS APPLIED MATERIALS & INTERFACES

Research Article

www.acsami.org

# Functionalized Nanoporous Polyethylene Derived from Miscible Block Polymer Blends

Toshinori Kato[†,‡,§] and Marc A. Hillmyer*[,‡]

[‡]Department of Chemistry, University of Minnesota, Minneapolis, Minnesota 55455, United States

[§]Tsukuba Research Center, Kuraray Co. Ltd., 41, Miyukigaoka, Tsukuba, Ibaraki, JAPAN 305-0841

Supporting Information

**ABSTRACT:** Functionalized nanoporous polyethylene (PE) was prepared through controlled introduction of thermoresponsive poly[2-(2-methoxyethoxy)ethyl methacrylate] ($PMe(OE)_2MA$), or poly{2-[2-(2-methoxyethoxy)ethoxy]-ethyl methacrylate} ($PMe(OE)_3MA$) onto the pore walls. The compatibility of polylactide (PLA) and $PMe(OE)_xMA$ ($x$ = 2, 3) was investigated by blending the corresponding homopolymers. The blends showed only one glass transition when the molar masses of both components were relatively low, whereas two glass transitions were observed in case of higher molar mass samples. $PMe(OE)_xMA$-*b*-PE-*b*-$PMe(OE)_xMA$ ($x$ = 2, 3) block polymers were synthesized by a combination of ring-opening metathesis polymerization, atom transfer radical polymerization, and hydrogenation. Those block polymer blends formed a disordered bicontinuous structure consisting of a mixed PLA/$PMe(OE)_xMA$ domain and a semicrystalline PE domain. The PLA component was selectively removed from those blends by mild base treatment. The resulting nanoporous polyethylene showed an improved water uptake as a result of the hydrophilic $PMe(OE)_xMA$ on the pore walls.

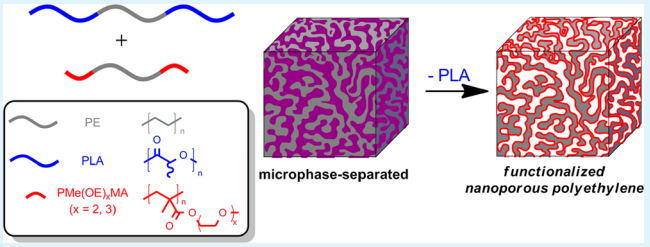


**KEYWORDS:** *nanoporous, polyethylene, hydrophilicity, thermoresponsive, block polymer blend, bicontinuous structure*

## INTRODUCTION

Block polymers containing an etchable block have received serious attention as precursors to nanoporous polymers.[1] Because nanoporous polymers have large internal surface areas, large pore volume, and uniform pore dimensions, these materials have been studied as separation/purification media,[2−5] battery separators,[6] templates for nanostructured materials,[7,8] low dielectric materials,[9−11] and low refractive index materials.[12] Since the pioneering study by Nakahama et al.,[13] a large number of methods for preparing nanoporous materials from block polymers containing an etchable block have been developed. One example of an easily etchable block is the aliphatic polyester polylactide (PLA),[14,15] and various block polymers containing PLA block have been reported as precursors for nanoporous polymers.[14,16−19]

For practical use of nanoporous polymers, both the pore wall functionality and the robustness of the matrix are important. In recent work, Rzayev et al. reported the preparation of nanoporous polystyrene (PS), in which the pore walls were lined with hydrophilic polydimethylacrylamide (PDMA), by etching PLA from a PLA-*b*-PDMA-*b*-PS triblock terpolymer.[20] The PDMA lining layer can be also converted to poly(acrylic acid) (PAA) by hydrolysis and to other polyacrylamides by sequential amine treatment. Guo et al. also reported an alternative method for preparing nanoporous PS with PAA lined pore walls.[21] Incorporation of olefin groups on the pore walls is also useful for subsequent functional group transformations.[22,23] For example, epoxy functionality on the pore wall derived from olefin groups was converted to an initiator for atom transfer radical polymerization (ATRP) and used for the surface graft polymerization of poly(ethylene glycol) methacrylate macromonomer (PEGMA) or 2-hydroxyethyl methacrylate (HEMA).[22] Another strategy to functionalize the pore walls is through the use of block polymer blends. For example, Mao et al. used PS-*b*-PLA/PS-*b*-poly(ethylene oxide) (PS-*b*-PEO) blends as a precursor.[24] In this system, PLA and PEO were miscible and formed a mixed phase in the PS matrix phase. PLA was selectively removed, but PEO remained intact on the pore wall. This nanoporous PS showed enhanced hydrophilicity compared to the parent nanoporous PS. Yang et al. also reported the fabrication of an ultrahigh density array of nanochannels from the blend which consistes of PS-*b*-poly(methyl methacrylate) (PMMA) with dicarboxylic acid end group and PMMA homopolymer.[25] PMMA homopolymer helps perpendicular orientation of PMMA cylindrical domain, then is removed by PMMA selective solvent to form pores. The resulting array of nanochannels have carboxylic groups on the pore walls.

Several approaches have also been taken to improve the mechanical robustness of nanoporous polymers. A cross-linking has been a technique widely applied, for example, by UV-irradiation,[26,27] thermal treatment,[28,29] ozone treatment,[30] use

Received: September 24, 2012
Accepted: December 14, 2012
Published: December 28, 2012

  

of radical initiators,[31,32] and other methods.[33−35] A thermoset system consisting of a monomer and a block polymer that has a reactive block with the monomer was also reported as a precursor for a robust nanoporous polymer.[16]

Polyethylene (PE) has appreciable mechanical properties, chemical resistance, and thermal resistance, making it an attractive matrix component for nanoporous polymers. A PE-*b*-PS that formed a bicontinuous microphase separated structure was converted to a bicontinuous nanoporous PE by the careful treatment with fuming nitric acid to etch the PS component.[36] A related approach using a PLA-*b*-PE-*b*-PLA was also reported in which a bicontinuous structure was formed by a simple hot press molding.[18] Such bicontinuous structures would be expected to show a high liquid flux because of the highly connected pores, and it could render the materials useful for filtration membranes and battery separators.

Here we report a nanoporous PE having pore walls lined with thermo-responsive polymer chains. First, we examined compatibility between PLA and poly[2-(2-methoxyethoxy)-ethyl methacrylate] ($PMe(OE)_2MA$) or poly{2-[2-(2-methoxyethoxy)ethoxy]ethyl methacrylate} ($PMe(OE)_3MA$). $PMe(OE)_xMA$ ($x$ = 2, 3) both show lower critical solution temperatures (LCST) in water at 26 °C ($x$ = 2) and 52 °C ($x$ = 3), respectively.[37] We prepared the polymer blends consisting of PLA and $PMe(OE)_2MA$ or $PMe(OE)_3MA$, and revealed that they gave miscible blends depending on their molar masses. The $PMe(OE)_xMA$-*b*-PE-*b*-$PMe(OE)_xMA$ ($^xOE^xO$) block polymers were successfully synthesized by the combination of ring-opening metathesis polymerization (ROMP) and ATRP followed by hydrogenation. The PLA-*b*-PE-*b*-PLA (LEL)/$^xOE^xO$ blends formed disordered, bicontinuous, and microphase separated structures. A selective PLA etching from the LEL/$^xOE^xO$ blends were successfully done and the resulting nanoporous PE monoliths showed better hydrophilicity compared to a nonfunctionalized nanoporous PE (Figure 1). This approach highlights the utility of the block polymer blends to enable a preparation of the mechanically robust and functional nanoporous polymers.

## RESULTS AND DISCUSSION

**Homopolymer Blends.** PLA and $PMe(OE)_xMA$ ($x$ = 2, 3) were prepared by tin catalyzed ring-opening polymerization of D,L-lactide and free radical polymerization of 2-(2-methoxyethoxy)ethyl methacrylate [$Me(OE)_2MA$] or 2-[2-(2-methoxyethoxy)ethoxy]ethyl methacrylate [$Me(OE)_3MA$] respectively. The polymers were codissolved in tetrahydrofuran (THF) and sequentially dried. We first tested the miscibility between PLA and $PMe(OE)_xMA$ ($x$ = 2, 3, Table 1) using differential scanning calorimetry (DSC). The thermograms for PLA-20, $PMe(OE)_3MA$-24 and their five blends are shown in Figure 2 (data also tabulated in Table S1 in the Supporting Informatiom).

Each of blends consisting of PLA-20 and $PMe(OE)_3MA$-24 showed only one glass transitions (Figure 2). The glass transition temperature ($T_g$) increased monotonically with increasing weight fraction of PLA ($w_{PLA}$) (Figure 3). These data are consistent with miscibility over the entire $w_{PLA}$ range. The $T_g$ dependence on the $w_{PLA}$ fits well with the Gordon−Taylor equation (eq 1).[38]

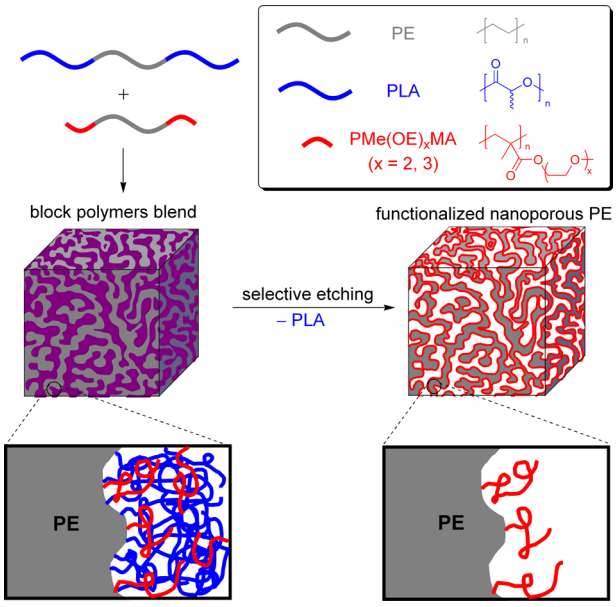


**Figure 1.** Preparation strategy of the nanoporous polyethylene whose pore wall is lined with $PMe(OE)_xMA$ ($x$ = 2, 3) by the PLA selective etching from the reactive block polymer blends.

**Table 1. Molecular Characteristics of Homopolymers**

| polymer | $M_n$ (kg/mol)[a] | $Đ$[a] |
|---|---|---|
| PLA-20 | 20 | 1.5 |
| PLA-61 | 61 | 1.3 |
| $PMe(OE)_2MA$-30 | 30 | 1.8 |
| $PMe(OE)_2MA$-77 | 77 | 2.5 |
| $PMe(OE)_3MA$-24 | 24 | 1.9 |
| $PMe(OE)_3MA$-62 | 62 | 2.4 |

[a]Number-average molar mass and polydispersity ($Đ$) were determined by the size exclusion chromatography (SEC) at 35 °C using a chloroform as the eluent and polystyrene standards.

$$T_{g,blend} = T_{g,PMe(OE)xMA} + k\left(\frac{w_{PLA}}{w_{PMe(OE)xMA}}\right)(T_{g,PLA} - T_{g,blend}) \quad (1)$$

Where $T_{g,i}$ and $w_i$ refers to the $T_g$ in K and the weight fraction of a component $i$, and $k$ is a fitting parameter. The fitting result with $k$ = 1.536 ($R^2$ = 0.981) is also shown in Figure 3. Also in case of the PLA-20/$PMe(OE)_2MA$-30 blend, only one glass transition was also observed (see Figure S1 and S2 in the Supporting Information). These results reflects the miscibility between PLA-20 and either $PMe(OE)_3MA$-24 or $PMe(OE)_2MA$-30.

On the other hand, for polymer blends prepared from the higher molar mass polymers, two $T_g$s were observed over the entire $w_{PLA}$ range. DSC traces for PLA-61, $PMe(OE)_3MA$-62, and their five blends are displayed in Figure 4a, and the corresponding derivative curves in Figure 4b. These data are consistent with phase separation and incompatibility between these higher molar mass PLA and $PMe(OE)_3MA$. By increasing the degree of polymerization of those polymers, the overall degree of segregation increased and thus macrophase separation occurred in the blends. The lower $T_g$ values slightly varied depending on the $w_{PLA}$, but the higher $T_g$ values showed little dependence on the $w_{PLA}$ [Figure 4a, b and Figure S3 in the


dx.doi.org/10.1021/am3020907 | ACS Appl. Mater. Interfaces 2013, 5, 291−300

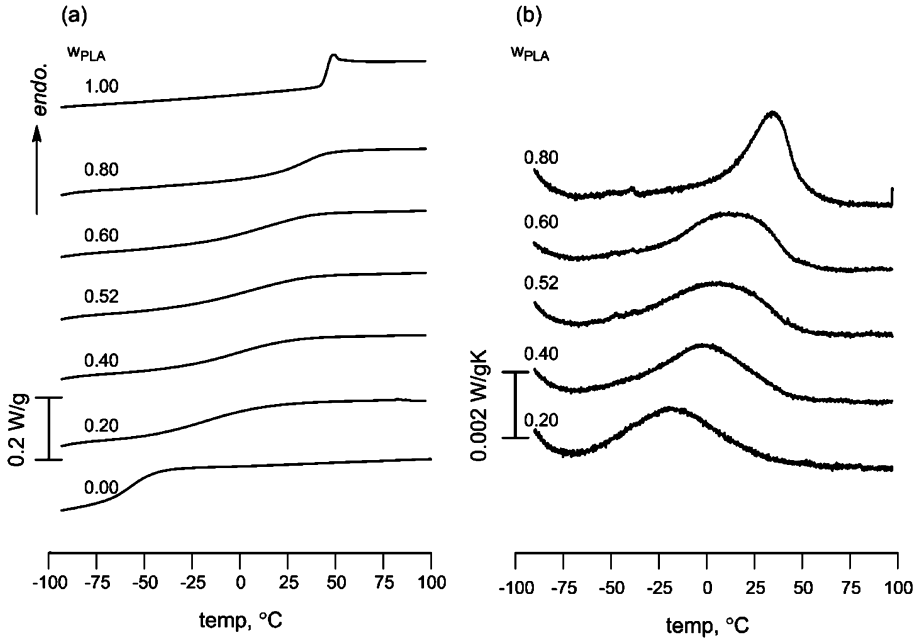


**Figure 2.** DSC traces for PLA-20, $PMe(OE)_3MA$-24, and indicated blends: (a) heat flow obtained at 10 °C/min, and (b) corresponding derivative curves for the blends.

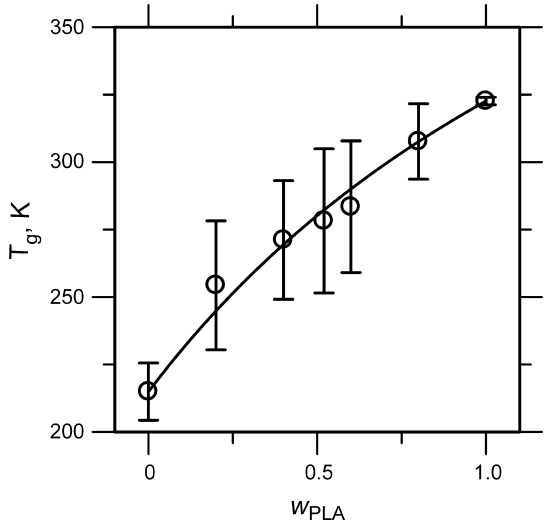


**Figure 3.** $T_g$ dependence on the weight fraction of PLA in the PLA-20/$PMe(OE)_3MA$-24 blends. The open circles are the experimental results and the error bars represent the observed glass transition widths. The solid curve corresponds to the Gordon−Taylor equation for $k$ = 1.536 ($R^2$ = 0.981).

Supporting Information]. This implies that this blend is a partially mixed and separated into a $PMe(OE)_3MA$-rich phase and a (mostly) PLA phase. A similar result was obtained in the PLA-60/$PMe(OE)_2MA$-72 blends (see Table S1 and Figures S4 and S5 in the Supporting Information).

**Synthesis of $^{x}OE^{x}O$.** The synthesis of $^{x}OE^{x}O$ was accomplished using the combination of ROMP, ATRP, and hydrogenation (Scheme 1).

Polycyclooctene (PCOE) with acetoxy end groups (AcO-PCOE-OAc) was synthesized by ROMP of *cis*-cyclooctene using the second. generation Grubbs catalyst and 1,4-diacetoxy-*cis*-2-butene as a chain transfer agent. The AcO-PCOE-OAc was transformed to PCOE with hydroxyl end groups (HO-PCOE−OH) using sodium metoxide.[18] The HO-PCOE-OH was quantitatively converted to a macroinitiator for ATRP of $Me(OE)_xMA$ by esterification with $\alpha$-bromoisobutyryl bromide (Br-PCOE-Br, Figure 5). Although, the number-average molar mass measured by SEC using chloroform as the eluent at 35 °C ($M_{n,\ SEC-CHCl3}$) changed during the chain end chemical modification, no apparent difference was observed in the number-average molar mass calculated from proton nuclear magnetic resonance ($^1$H NMR) spectroscopy ($M_{n,\ NMR}$) (Table 2). The change in $M_{n,\ SEC-CHCl3}$ could be due to the interaction between the SEC column packing and the chain end hydroxyl groups as pointed out elsewhere.[39]

$PMe(OE)_3MA$-*b*-PCOE-*b*-$PMe(OE)_3MA$ ($^3OC^3O$) was synthesized by the ATRP of $Me(OE)_3MA$ using Br-PCOE-Br as a macroinitiator. Copper(I) chloride was selected as a catalyst for the halogen exchange technique[40−42] to ensure that high block efficiency was achieved. The polymerization of $Me(OE)_3MA$ was quenched at the conversion of 30% (50 h). The SEC curve shows high molar mass shift keeping the unimodal shape after the ATRP of $Me(OE)_3MA$ consistent with a successful triblock formation (Figure 6). ATRP of $Me(OE)_2MA$ was also successful (see Figure S6 in the Supporting Information).

$^3OE^3O$ was synthesized by hydrogenation of $^3OC^3O$ using *p*-toluenesulfonyl hydrazide/tri*n*-propyl amine (*p*-$TsNHNH_2$/$nPr_3N$) as a hydrogenation reagent.[43] No residual C═C double bonds were detected by $^1$H NMR analysis (Figure 7). In SEC measurement of $^3OE^3O$ at 135 °C using 1,2,4-trichlorobenzene (TCB) as the eluent, there was a large low molar mass shoulder peak besides the main peak (not shown). The $^3OC^3O$, which showed unimodal SEC curve at 35 °C using chloroform as the eluent (Figure 6), also gave a similar large low molar mass shoulder peak on SEC measurement at 135 °C with TCB as the eluent (not shown). In case of the HO-PE-OH, which was derived from the HO-PCOE-OH by a hydrogenation and did not have any $PMe(OE)_xMA$ ($x$ = 2, 3) component, no low molar mass shoulder appeared on SEC at 135 °C (see Figure S7 in the Supporting Information). So, the low molar mass

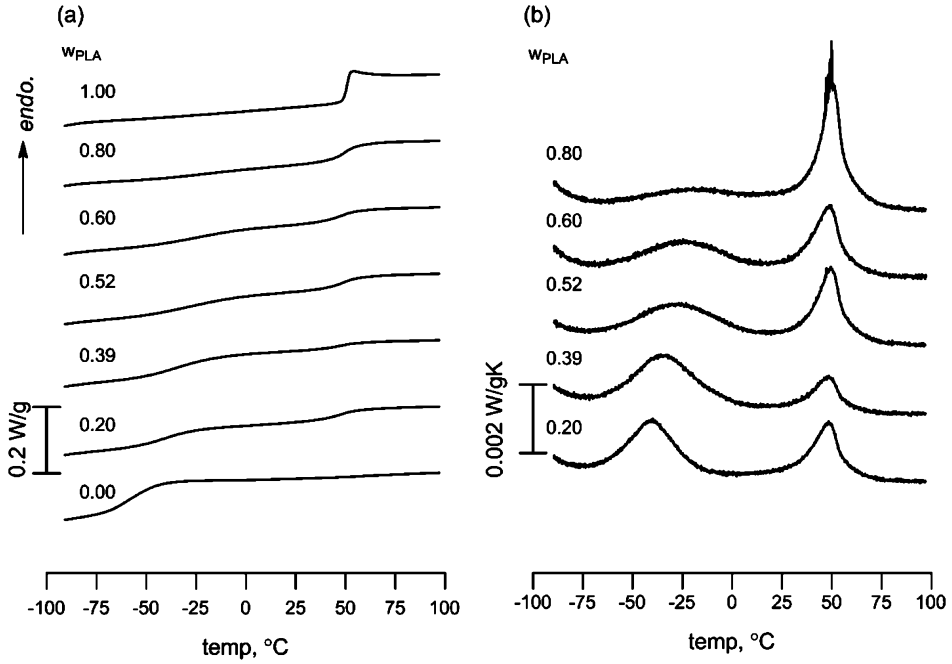


**Figure 4.** DSC traces for the PLA-61, the $PMe(OE)_3MA$-62, and the indicated blends: (a) heat flow obtained at 10 °C/min, and (b) corresponding derivative curves.

**Scheme 1. Synthesis of $^{x}OE^{x}O$**

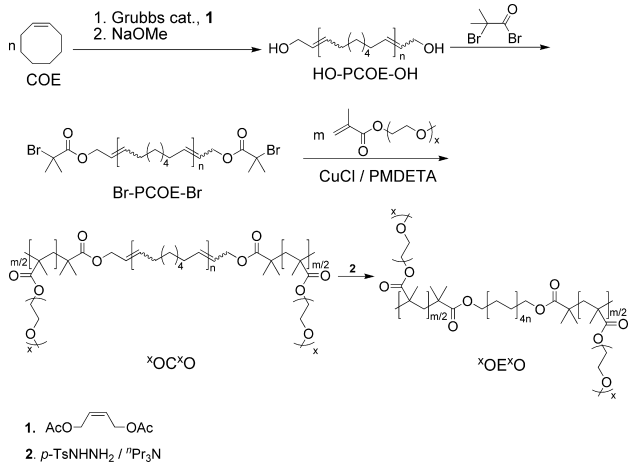


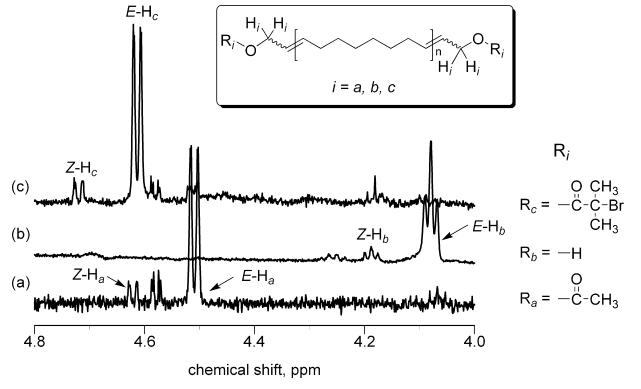


**Figure 5.** $^1$H NMR spectra for the polymer chain end region for (a) the AcO-PCOE-OAc, (b) the HO-PCOE-OH, and (c) the Br-PCOE-Br in $CDCl_3$ at room temperature.

**Table 2. Molar Mass and Characteristics of (Co)polymers**

| | molar Mass | | | |
|---|---|---|---|---|
| | SEC (35 °C, $CHCl_3$)[a] | | $^1$H NMR | |
| polymer | $M_{n,\ SEC-CHCl3}$ (kg/mol) | Đ[b] | $M_{n,\ NMR}$[c] (kg/mol) | weight fraction $w_{PMe(OE)xMA}$[d] |
| AcO-PCOE-OAc | 48.9 | 1.61 | 29.3 | |
| HO-PCOE-OH | 45.3 | 1.68 | 29.2 | |
| Br-PCOE-Br | 49.3 | 1.75 | 28.8 | |
| HO-PE-OH | | | 29.0 | |
| $^2OC^2O$ | 107 | 1.56 | 65.1 | 0.56 |
| $^2OE^2O$ | | | 66.8 | 0.56 |
| $^3OC^3O$ | 78.6 | 1.80 | 40.6 | 0.29 |
| $^3OE^3O$ | | | 40.9 | 0.28 |

[a]Determined using PS standards. [b]Polydispersity. [c]Determined by $^1$H NMR end-group analysis for PCOEs based on the assumption that all polymer chains have two functional groups at the both ends. $M_{n,\ NMR}$ of block polymer was calculated by devided the $M_{n,\ NMR}$ of the PCOE or PE block by $(1 - w_{PMe(OE)xMA})$. [d]Weight fractions of $PMe(OE)_xMA$ ($x$ = 2, 3) were calculated by $^1$H NMR spectroscopy.

shoulder observed in $^3OC^3O$ and $^3OE^3O$ on SEC at 135 °C might have been due to interactions between the $PMe(OE)_3MA$ component and the column packing. When the homopolymer $PMe(OE)_xMA$ (x = 2, 3) was tested with this apparatus, no peaks were observed possibly due to adsorption by the column packing material. It might support the undesirably strong interaction between $PMe(OE)_xMA$ components and the column packing. By these results, the SEC measurement at 135 °C was not reliable for the polymers containing the $PMe(OE)_xMA$ components.

The weight fraction of the $PMe(OE)_3MA$ component ($w_{PMe(OE)3MA}$) in those block polymers (i.e., $^3OC^3O$ and $^3OE^3O$) were estimated as 0.290 and 0.284 by $^1$H NMR measurements, respectively. During the purification process of


dx.doi.org/10.1021/am3020907 | ACS Appl. Mater. Interfaces 2013, 5, 291−300

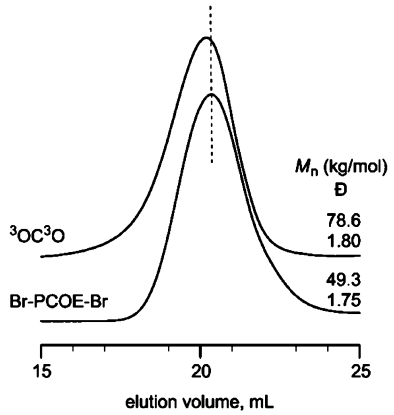


**Figure 6.** SEC curves measured at 35 °C using chloroform as the eluent for the Br-PCOE-Br, and the $^3$OC$^3$O. Molar masses are relative to polystyrene standards. The dashed line has been added at the peak top of the Br-PCOE-Br SEC curve to guide the eye.

$^3$OE$^3$O, it was reprecipitated using an excess amount of acetone which is a good solvent for homo PMe(OE)$_3$MA.[35] If a chain scission had occurred in PMe(OE)$_3$MA block during the hydrogenation process, it would have generated homo PMe(OE)$_3$MA and this homo PMe(OE)$_3$MA should have been removed in the precipitation process. It should have caused a change of $w_{PMe(OE)3MA}$ between $^3$OC$^3$O and $^3$OE$^3$O. Experimentally, almost no change was observed in $w_{PMe(OE)3MA}$ between $^3$OC$^3$O and $^3$OE$^3$O post precipitation, and we concluded that the hydrogenation proceeded as designed without significant PMe(OE)$_3$MA chain scission or decomposition. These results supported the successful synthesis of $^3$OE$^3$O. Nearly identical results were obtained for the $^2$OE$^2$O synthesis (see Figure S6 and S8 in the Supporting Information)

**Preparation of Nanoporous Polyethylene.** LEL, a precursor to a nanoporous polyethylene, was synthesized by ring-opening polymerization of D,L-lactide using the same HO-PE-OH, which was derived from the HO-PCOE-OH, as described above as a macroinitiator.[18] The number-average molar mass and the $w_{PLA}$ of the LEL sample were 88.4 kg/mol and 0.60 respectively as estimated from $^1$H NMR spectroscopy (see Figure S9 in the Supporting Information), respectively. The polydispersity (Đ) estimated from the SEC measurement at 135 °C was 1.37 (see Figure S7 in the Supporting Information).

The LEL and $^3$OE$^3$O blend (1.0/0.1 w/w) was prepared through a codissolution of the block polymers in xylenes at 140 °C, followed by evaporation of the solvent at atmospheric pressure in air at the same temperature. To avoid a potential disturbance of the desired bicontinuous morphology, low levels of $^x$OE$^x$O were utilized. The samples were further dried under reduced pressure at 70 °C for two days to ensure removal of residual solvent and then melt molded to give a 1 mm-thick disks using a hot press at 165 °C.

Individual small-angle X-ray scattering (SAXS) measurement of the melt molded LEL and $^3$OE$^3$O were performed. Data was corrected by Lorentz factor (i.e., $q$ vs $Iq^2$, where $q$ is the scattering vector and $I$ is the observed scattering intensity).[44] The SAXS profile of LEL [Figure 8(a)] exhibited a primary peak at about $q^* = 0.083$ nm$^{-1}$ and a broad peak around $q = 0.3$ nm$^{-1}$. The primary peak reflects a microphase separation structure whose $d$-spacing ($d^*$) is about 76 nm, and the other peak may indicate a periodic crystalline−amorphous layer structure[45] in the PE phase with an average $d$-spacing of about 21 nm. An additional shoulder peak also emerged at around $q$

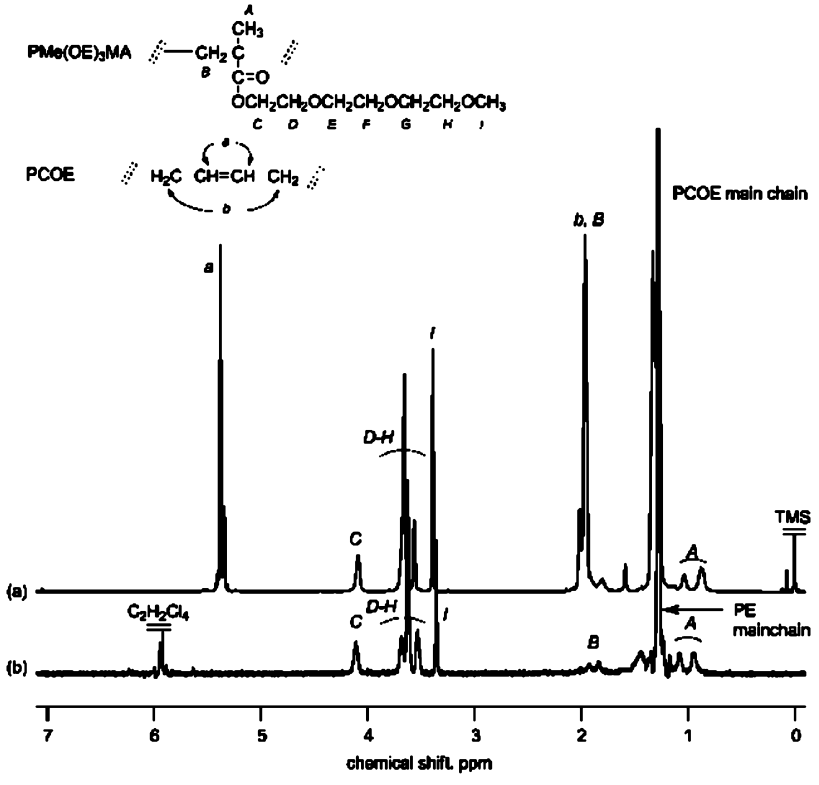


**Figure 7.** $^1$H NMR spectra for (a) the $^3$OC$^3$O in $CDCl_3$ at room temperature, and (b) the $^3$OE$^3$O in $C_2D_2Cl_4$ at 130 °C.

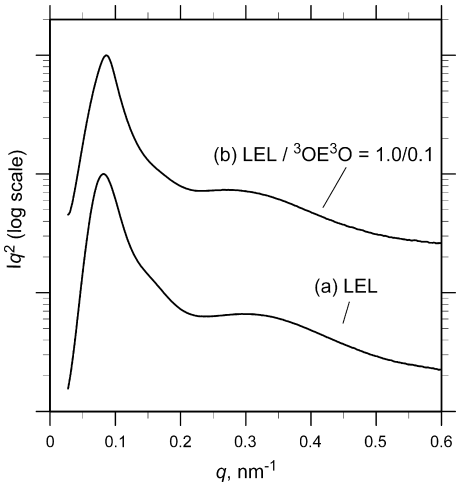


**Figure 8.** One-dimensional SAXS profiles for (a) the LEL, and (b) the LEL/$^3$OE$^3$O blend (1.0/0.1 w/w) at room temperature. Profiles have been vertically shifted for a comparison.

$\approx 2q^*$. As no further higher-order peak was observed, this might reflect a local PE-PLA periodic structure. Consistent with our previous results, LEL forms a disordered microphase separated structure.[18] As further evidence, the structure of LEL and etched LEL were also analyzed by SAXS and scanning electron microscopy (SEM) (see Figure S10A, B in the Supporting Information). The SEM observation of etched LEL clearly showed a bicontinuous pore structure. SAXS profiles were comparable with those of LEL and LEL/$^3$OE$^3$O blend. From these results, we concluded that LEL and LEL/$^3$OE$^3$O blneds also adopted a disordered bicontinuous microphase separated structure. The SAXS profiles for $^2$OE$^2$O and $^3$OE$^3$O are shown in Figure S11 in the Supporting Information and they indicate those block polymer also have microphase separated structure. The $d^*$ for LEL, $^3$OE$^3$O, and their blend are given in Table 3, which indicates that no significant disturbance in the morphology of LEL occurred by the addition of $^3$OE$^3$O.

Confirmed by SEM analysis (Figure 11), etched LEL/$^3$OE$^3$O blend clearly has a bicontinuous pore structure. Additionally, etched LEL/$^3$OE$^3$O gave a similar SAXS profile with that of LEL/$^3$OE$^3$O blend (Figure 12). We concluded that the bicontinuous microphase separated structure was kept during the etching process from this result.

**Table 3. Characteristics of the nanoporous polyethylenes and their precursor**

| | before etching | after etching | | | |
|---|---|---|---|---|---|
| | | | | total pore volume (mL/g) | |
| sample | $d^*$ (nm) | $d^*$ (nm) | $r_{pore}$ (nm)[a] | observed[b] | theoretical[c] |
| LEL | 76.0 | 70.6 | 18.3 | 0.905 | 1.20 |
| $^3$OE$^3$O | 37.5 | | | | |
| $^2$OE$^2$O | 49.6 | | | | |
| LEL/$^3$OE$^3$O | 73.2 | 71.9 | 13.6 | 0.364 | 0.960 |
| LEL/$^2$OE$^2$O | 76.0 | 76.0 | 15.9 | 0.229 | 0.960 |

[a]The peak radius of the pores evaluated by the BJH analyses of the nitrogen desorption isotherm at 77K. [b]The pore volume calculated from the volume of the absorbed nitrogen at $P/P_0 \sim 0.975$ on the desorption measurement. [c]Estimated using the density values as $d_{PE}$ [46] = 0.95 g/cm$^3$, $d_{PLA}$ [47] = 1.25 g/cm$^3$ and $d_{PMe(OE)xMA}$ [45] = 1.19 g/cm$^3$.

Figure 9 shows DSC traces for LEL and LEL/$^3$OE$^3$O blends. The $T_g$ of the phase including PLA shifted to lower

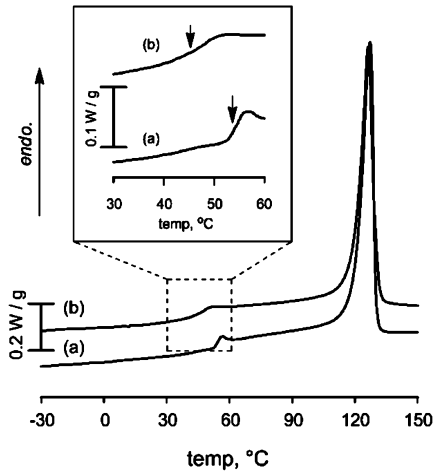


**Figure 9.** DSC traces for (a) the LEL, and (b) the LEL/$^3$OE$^3$O blend (1.0/0.1 w/w). All traces was recorded on the first. heating at the rate of 10 °C/min after cooling to −90 °C.

temperature, but no prominent change occurred in the PE melting peak at 130 °C. The SAXS and the DSC results indicate that PLA and PMe(OE)$_3$MA formed a single phase based on their miscibility and this phase was separated from the PE phase.

The etched LEL/$^3$OE$^3$O was dissolved in tetrachloroethane-$d_4$ and analyzed by $^1$H NMR spectroscopy. Figure 10 shows a

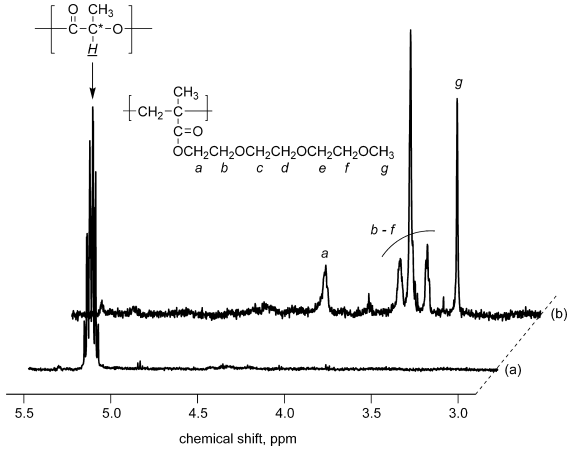


**Figure 10.** $^1$H NMR spectra for (a) the LEL and (b) the etched LEL/$^3$OE$^3$O blend in $C_2D_2Cl_4$ at 130 °C.

comparison of the $^1$H NMR spectra for LEL and the etched LEL/$^3$OE$^3$O blend. The PLA methine proton signals at 5.24 ppm (Figure 10a) were not present in the $^1$H NMR spectrum of an etched LEL/$^3$OE$^3$O sample. On the other hand, the resonances related to both the main chain and the side chain of the PMe(OE)$_3$MA were observed clearly (Figure 10b). The PMe(OE)$_3$MA weight fraction in the etched LEL/$^3$OE$^3$O sample was calculated as 0.06 from a peak integration in the $^1$H NMR spectrum. This value agreed well with the theoretical

value (0.06), which supports that PMe(OE)$_3$MA is retained in the nanoporous polyethylene.

The SEM image of the etched sample of the LEL/$^3$OE$^3$O blend is shown in Figure 11; a disordered bicontinuous

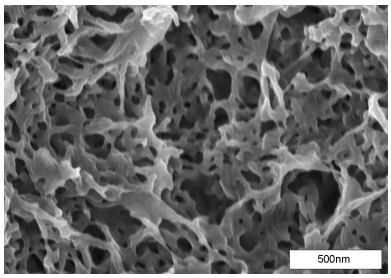


**Figure 11.** SEM image of the cryo-fractured surface of the etched LEL/$^3$OE$^3$O blend. The sample was coated with Pt (about 2 nm thick).

structure originating from the microphase precursor is evident. Additionally, no drastic change or significant $q^*$ shift in the SAXS profiles (Figure 12, Table 3) was observed between the

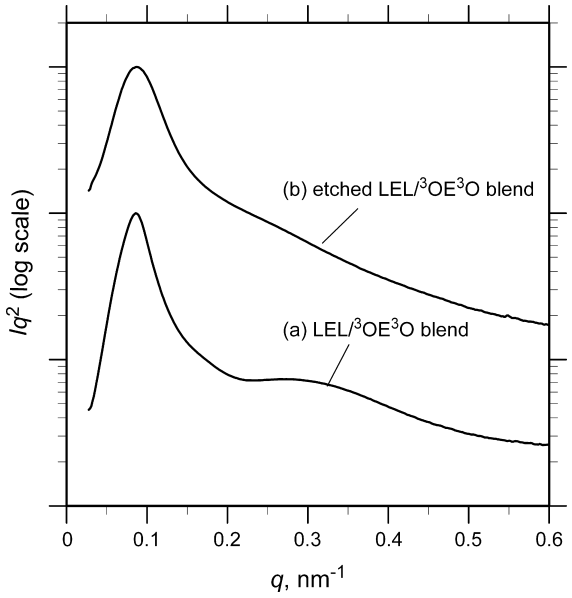


**Figure 12.** One-dimensional SAXS profiles for (a) unetched, and (b) etched LEL/$^3$OE$^3$O blend (1.0/0.1 w/w).

unetched and the etched LEL/$^3$OE$^3$O blend. These results confirm that the microphase separated and bicontinuous structure was retained during the etching.

The nitrogen adsorption/desorption isotherms at $T$ = 77 K, the pore-size distribution of the etched LEL/$^3$OE$^3$O blend, and the estimated peak pore radius ($r_{pore}$) are shown in Figure 13 and Table 3, respectively. The total pore volume calculated at $P/P_0 \sim 0.975$ (corresponding to the pores whose radius are less than about 40 nm) are also shown in Table 3. The isotherms are of type IV shape and it indicates the existence of mesopores in the etched LEL/$^3$OE$^3$O. The $r_{pore}$ was 13.6 nm and a narrow pore-size distribution was obtained.

Because the density of PMe(OE)$_x$MA is not reported, we assumed that the density of the PMe(OE)$_3$MA is same with that of poly(methyl methacrylate) ($d_{PMMA}$ = 1.19 g/mL). The PLA volume fraction in the LEL/$^3$OE$^3$O blend was roughly

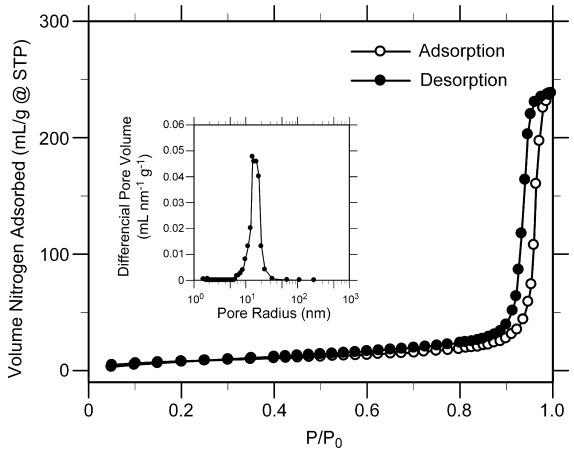


**Figure 13.** Nitrogen adsorption measurement on the etched LEL/$^3$OE$^3$O blend measured at $T$ = 77 K showing the adsorption (unfilled circles) and the desorption (filled circles) isotherms with the inset showing the average pore size distribution calculated using the BJH method from the desorption data.

estimated as 0.96 mL/g based on this assumption. The observed total pore volume (0.364 mL/g) was less than the estimated value. The narrow pore radius distribution (the inlet in Figure 13) implies that the etched LEL/$^3$OE$^3$O blend has almost no pores larger than 100 nm radius, so some pores might have collapsed during the etching process. The partial pore collapse was also observed in the case of the pure LEL (Table 3) in spite of the narrow pore distribution (see Figure S13 in the Supporting Information).

The effect of the introducing PMe(OE)$_3$MA to the pore wall was investigate by measuring the water uptake as a function of temperature. The two nanoporous PEs (etched LEL, and the LEL/$^3$OE$^3$O blend) were placed in two separate vials containing water kept at 70 °C for 1h. Then nanoporous PEs were retrieved from the vials and the surface was quickly wiped with a fine tissue paper. The samples were then quickly weighed. Then the temperature was changed and the water uptake volume was observed at 55, 40, and 0 °C in the same manner (Figure 14).

The water uptake change was very low for the etched LEL because of a highly hydrophobic nature of PE. However, once PMe(OE)$_3$MA was incorporated to the nanoporous PE, the water uptake was dramatically increased even at 70 °C which was higher than the reported LCST[35] of PMe(OE)$_3$MA–water system (52 °C). The water uptake volume at 70 and 0 °C are 0.432 and 0.465 mL/g, respectively. Those value are moderately comparable with the total pore volume (0.364 mL/g) observed in the nitrogen desorption measurement; however, we were unable to collect enough data for a full statistical analysis of the differences. This implies that PMe(OE)$_3$MA was more hydrophilic than the PE surface even at the temperature over the LCST of PMe(OE)$_3$MA and enough to facilitate the water uptake. While we expected a water uptake change for the LEL/$^3$OE$^3$O blend around the LCST of PMe(OE)$_3$MA-water system, the water uptake was not clear between 55 and 40 °C. The water uptake for etched LEL/$^2$OE$^2$O is also tested and shown in Figure S19 in the Supporting Information. These tests show improved hydrophilicity, but may not be suitable for evaluating thermal-responsiveness. The temperature dependence of hydrophilicity


dx.doi.org/10.1021/am3020907 | ACS Appl. Mater. Interfaces 2013, 5, 291–300

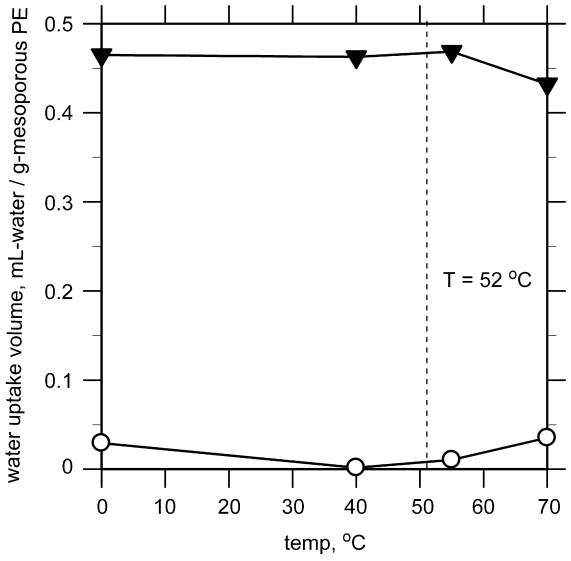


**Figure 14.** Temperature dependence of the water uptake for (a) the etched LEL (open circles), and (b) the etched LEL/$^{3}$OE$^{3}$O blend (filled inverted triangles). The dashed line on $T$ = 52 °C that indicates a reported LCST[35] for PMe(OE)$_3$MA has been added to guide the eye.

will be evaluated by water flux measurement of membranes made of those materials in future work.

## CONCLUSIONS

The miscibility between PLA and PMe(OE)$_x$MA was investigated and the molecular weight dependence of the miscibility was clarified in both $x$ = 2 and 3. The synthesis of the PMe(OE)$_x$MA-*b*-PE-*b*-PMe(OE)$_x$MA ($x$ = 2, 3) was achieved using ROMP, ATRP, and hydrogenation combination. The block polymer blends with PLA-*b*-PE-*b*-PLA were prepared and formation of the disordered bicontinuous structure comprised of the PLA–PMe(OE)$_x$MA miscible phase and the PE phase was observed. The PLA component was selectively etched out from those blends by a mild base treatment, while the PMe(OE)$_x$MA remained in the resulting nanoporous PE. The effect of incorporation of PMe(OE)$_x$MA to the pore wall was confirmed by the water uptake test.

## EXPERIMENTAL SECTIONS

**Materials.** Unless specifically noted, all chemicals were used as received from Aldrich. Dichloromethane, toluene, and tetrahydrofuran (THF) were passed through alumina columns and thoroughly degassed. D,L-Lactide (99%, Purac), was recrystallized twice from ethyl acetate and dried under vacuum before being stored into a glovebox under a $N_2$ atmosphere. Tin(II) 2-ethylhexanoate [Sn(oct)$_2$, 95%, Aldrich] was distilled using Kugelrohr apparatus under reduced pressure and stored under $N_2$. 2-(2-Methoxyethoxy) ethyl methacrylate (97%, TCI Chemical) was distilled from $CaH_2$ under reduced pressure before use. Tri(ethylene glycol) monomethyl ether (95%, Aldrich) was dried over $CaH_2$ and distilled under reduced pressure. 2-[2-(2-methoxyethoxy)ethoxy]ethyl methacrylate was synthesized as previously reported[35] and distilled from $CaH_2$ under reduced pressure before use. 2,2′-azobis(isobutyronitrile) (98%, Aldrich) was recrystallized from methanol and stored at −20 °C. *cis*-Cyclooctene (95%, Acros) and *cis*-1,4-diacetoxy-2-butene (95%, TCI Chemical) were distilled from $CaH_2$ under an argon atmosphere before use. Copper(I) chloride (99.995%, Aldrich) was purified with glacial acetic acid, washed with pure ethanol, dried under reduced pressure, and stored in a nitrogen atmosphere. Silica gel powder (Mallinckrodt, grade-62) used as an adsorbent for a residual copper catalyst from an reaction solution of ATRP was used as received. AcO-PCOE-OAc, HO-PCOE−OH, HO-PE−OH and PLA-*b*-PE-*b*-PLA (LEL) were synthesized following a reported procedure.[18] The PLA was synthesized using benzyl alcohol as an initiator and Sn(oct)$_2$ as a catalyst in toluene at 90 °C. The PMe(OE)$_x$MA ($x$ = 2,3) were synthesized by conventional free radical polymerization using AIBN as a radical initiator and dodecane thiol as a chain transfer agent in toluene at 60 °C.

**Characterization.** $^{1}$H NMR spectra obtained using $CDCl_3$ solvent at room temperature were recorded on a Varian Inova 500 operating at 500 MHz, spectra obtained using tetrachloroethane-$d_4$ solvent at 130 °C were recorded on a Bruker Avance III 500 operating at 500 MHz. Size exclusion chromatography (SEC) of analyte that were soluble in chloroform was conducted using a Hewlett −Packard (Agilent Technologies) instrument equipped with a Hewlett-Packard 1047A refractive index detector. Samples were prepared in $CHCl_3$ (mobile phase) and passed through three PLgel 5 μm Mixed-C columns (Agilent Technologies) in series at a constant flow rate and temperature (1.0 mL/min at 35 °C).

SEC at 135 °C was conducted using a Polymer Laboratories GPC-220 liquid chromatograph. Samples were prepared in 1,2,4-trichlorobenzene (mobile phase, including 0.0125% of butylated hydroxy toluene) and passed through three PIGel 10 μm Mixed-B columns (Agilent Technology) at a constant flow rate and temperature (1.0 mL/min at 135 °C). Both SEC instruments were calibrated using PS standards (Polymer Laboratories).

Differential scanning calorimetric (DSC) measurements for homopolymer blends were performed using a DSC Q-1000 calorimeter from TA Instruments calibrated using an indium standard. Homopolymer blend samples for the DSC measurement were prepared by dissolving together the appropriate polymers in THF. The solution was sequentially cast into a Petri dish, then dried under reduced pressure at room temperature overnight. Each samples hermetically sealed in aluminum pans was heated to 200 °C at the rate of 10 °C/min and annealed at 200 °C for 10 min to remove their thermal history in DSC chamber. They were subsequently cooled to −100 °C min$^{-1}$, maintained at 100 °C for 2 min, then heated to 100 °C at the rate of 10 °C/min; all thermal events are recorded on this heating cycle. Differential scanning calorimetry measurements of block polymer and block polymer blend samples were conducted on a TA Instruments Discovery DSC calibrated with an indium standard. Block polymer blend samples were prepared by dissolving the appropriate mixture of block polymers in hot xylenes. These solutions were then cast into a Petri dish at 140 °C. The blend samples were dried under reduced pressure at 70 °C for 2 days, and then melt pressed at 165 °C using a metal mold to form a 1 mm thick disk. A small piece of this melt pressed disk was used for DSC measurement. Block polymer blend samples hermetically sealed in aluminum pans were cooled to −90 °C, this temperature was maintained for 2 min, at which time the samples were heated to 180 °C at the rate of 10 °C min$^{-1}$.

Small-angle X-ray scattering (SAXS) experiments were performed at the Advanced Photon Source (APS) at Argonne National Laboratories Sector 5-ID-D maintained by the DuPont-Northwestern-Dow Collaborative Access Team (DND-CAT). The X-ray wavelength was 0.7294 Å. Scattering intensity was monitored using a Mar 165 diameter CCD detector with a resolution of 2048 × 2048. The two-dimensional scattering patterns were azimuthally integrated to afford one-dimensional profiles presented as spatial frequency ($q$) versus scattered intensity.

Scanning electron microscopy was performed on a Hitachi S-4700 FE-SEM operating at 3.0 kV accelerating voltage. Samples were prepared by fracturing bulk samples that had been immersed in liquid $N_2$ for 10 min. Before imaging, a platinum coating approximately 2 nm thick was applied using a VCR high-resolution indirect ion-beam sputtering system. Nitrogen adsorption/desorption measurements were carried out at 77 K using a Quantachrome autosorb iQ system. The specific surface area of the nanoporous PE was calculated using the Brunauer–Emmet–Teller method;[49] the pore-size distribution were determined using the Barret–Joyner–Halenda model.[50]

**Synthesis of Br-PCOE-Br Macroinitiator.** $\alpha$-Bromoisobutyryl bromide (1.15 g; 5 mmol) was added dropwise to a solution of HO-PCOE−OH (5.0g; 0.34 mmol OH), triethylamine (0.25 g; 2.5 mmol), and dichloromethane (50 mL) in a dried 100 mL round-bottom flask while stirring at room temperature under argon atmosphere. The reaction mixture was stirred for 1 h and then poured into a large excess of cold methanol to precipitate Br-PCOE-Br (5.0 g, 100%). The resulting polymers were further purified by reprecipitation in a THF/methanol system and freeze-dried from a solution of benzene.

**General Procedure for the ATRP of Me(OE)$_x$MA ($x$ = 2,3) with the Br-PCOE-Br Macroinitiator.** The macroinitiator (Br-PCOE-Br), CuCl, *N*, *N*, *N*′, *N*′, *N*″-pentamethyldiethylenetriamine (PMDETA), toluene, and Me(OE)$_x$MA monomer were added to a dried 50 mL Schlenck flask equipped with magnetic stir bar and stirred untilled completely dissolved. A molar ratio of $[C-Br]_0$: $[CuCl]_0$: $[PMDETA]_0$ (1:1:2) and monomer concentration $[Me(OE)_xMA]_0$ (1.5 mol/L) were kept constant in all ATRP experiments. The reagent mixture was degassed by three freeze−pump−thaw cycles, then backfilled with argon. The flask was immersed in an oil bath warmed to 80 °C. During the polymerization, samples were periodically removed using a syringe while maintaining an argon atmosphere; $^1$H NMR was used to determine the monomer conversion of each sample. When the conversion reached a desired value, the flask was cooled with ice/water and exposed to air to terminate the polymerization. The reaction mixture was diluted with $CH_2Cl_2$, and silica gel powder was added to the mixture. The mixture was stirred for about 20 min and filtered using a glass filter to remove the silica gel and adsorbed copper catalyst. The filtrate was concentrated under reduced pressure, then poured into a large excess of cold methanol. The resulting polymer, PMe(OE)$_x$MA-*b*-PCOE-*b*-PMe(OE)$_x$MA ($^x$OC$^x$O) was further purified by reprecipitation in THF/methanol system and freeze-dried from a solution of benzene.

**General Procedure for Hydrogenation of the $^x$OC$^x$O.** Hydrogenation of $^x$OC$^x$O was carried out using *p*-toluenesulfonyl hydrazide (*p*-TsNHNH$_2$)/tri *n*-propyl amine ($n$Pr$_3$N) system.[41] $^x$OC$^x$O, *p*-TsNHNH$_2$, butylated hydroxy toluene (BHT, 20 ppm vs $^x$OC$^x$O), and xylenes (isomer mixture) were added to a dried round-bottom flask equipped with a magnetic stir bar and a reflux condenser. The mixture was purged with bubbling argon for 15 min and then $n$Pr$_3$N was added. A molar ratio of $[C{=}C]_0$:$[p\text{-TsNHNH}_2]_0$: $[n\text{Pr}_3\text{N}]_0$ (1:5:5) and a polymer concentration of 20g/L was used. The mixture was heated to 140 °C for 4 h, and then poured to a large excess of cold hexanes to precipitated resulting polymer, PMe-(OE)$_x$MA-*b*-PE-*b*-PMe(OE)$_x$MA ($^x$OE$^x$O). The resulting polymer was further purified by reprecipitation from hot toluene in cold acetone system and dried at 50 °C for 2 days under reduced pressure.

**Preparation of Nanoporous PE.** Hot press molded disk (1 mm thickness) of the LEL or the LEL/$^x$OE$^x$O blend was cut into small pieces and immersed in 0.5 M NaOH in methanol/water mixture (40/60 v/v) for 3 days at 50 °C. It was cooled to room temperature and then washed, first with a methanol−water mixture and then with pure methanol. The washed nanoporous PE was dried for 24 h in vacuo at 40 °C.

## ■ ASSOCIATED CONTENT

### Ⓢ Supporting Information

Figures S1−S19 and Table S1. This material is available free of charge via the Internet at http://pubs.acs.org.

## ■ AUTHOR INFORMATION


### Corresponding Author

*E-mail: hillmyer@umn.edu.

### Present Address

†Kuraray Research & Technical Center, Kuraray America, Inc., 11500 Bay Area Blvd., Pasadena, TX 77507


### Notes

The authors declare no competing financial interest.

## ■ ACKNOWLEDGMENTS

This work was supported by Kuraray Co. Ltd. Parts of this work were carried out in the Institute of Technology Characterization Facility, University of Minnesota, which receives partial support from NSF through the MRSEC program. SAXS measurements were performed at the DuPont-Northwestern-Dow Collaborative Access Team (DND-CAT) located at Sector 5 of the Advanced Photon Source (APS). DND-CAT is supported by E. I. DuPont de Nemours & Co., The Dow Chemical Company, and the State of Illinois. Use of the APS, and Office of Science User Facility operated for the U.S. Department of Energy (DOE) Office of Science by Argonne National Laboratory, was supported by the U.S. DOE under Contract DE-AC02-06CH11357. The authors thank Dr. Louis M. Pitet and Dr. Myungeun Seo for helpful discussion for preparing a nanoporous polymer.

## ■ REFERENCES


(1) Olson, D. A.; Chen, L.; Hillmyer, M. A. *Chem. Mater.* **2008**, *20*, 869−890.

(2) Yang, S. Y.; Ryu, I.; Kim, H. Y.; Kim, J. K.; Jang, S. K.; Russell, T. P. *Adv. Mater.* **2006**, *18*, 709−712.

(3) Uehara, H.; Kakiage, M.; Sekiya, M.; Sakuma, D.; Yamanobe, T.; Takano, N.; Barraud, A.; Meurville, E.; Ryser, P. *ACS Nano* **2009**, *3*, 924−932.

(4) Phillip, W. A.; Amendt, M.; O'Neill, B.; Chen, L.; Hillmyer, M. A.; Cussler, E. L. *ACS Appl. Mater. Interfaces* **2009**, *1*, 472−480.

(5) Li, L.; Szewczykowski, P.; Clausen, L. D.; Hansen, K. M.; Jonsson, G. E.; Ndoni, S. *J. Membr. Sci.* **2011**, *384*, 126−135.

(6) Wong, D. T.; Mullin, S. A.; Battaglia, V. S.; Balsara, N. P. *J. Membr. Sci.* **2012**, *394 - 395*, 175−183.

(7) Thurn-Albrecht, T.; Schotter, J.; Kästle, G. A.; Emley, N.; Shibauchi, T.; Krusin-Elbaum, L.; Guarini, K.; Black, C. T.; Tuominen, M. T.; Russell, T. P. *Science* **2000**, *290*, 2126−2129.

(8) Johnson, B. J. S.; Wolf, J. H.; Zalusky, A. S.; Hillmyer, M. A. *Chem. Mater.* **2004**, *16*, 2909−2917.

(9) Fu, G. −D.; Yuan, Z.; Kang, E.-T.; Neoh, K.-G.; Meiying, D.; Lai, M.; Huan, A. C. H. H. *Adv. Funct. Mater.* **2005**, *15*, 315−322.

(10) Chung, C.-M.; Lee, J.-H.; Cho, S.-Y.; Kim, J.-G.; Moon, S.-Y. *J. Appl. Polym. Sci.* **2006**, *101*, 532−538.

(11) Bucholz, T. L.; Li, S. P.; Loo, Y. −L. *J. Mater. Chem.* **2008**, *18*, 530−536.

(12) Ndoni, S.; Li, L.; Schulte, L.; Szewczykowski, P. P.; Hansen, T. W.; Guo, F.; Berg, R. H.; Vigild, M. E. *Macromolecules* **2009**, *42*, 3877−3880.

(13) Lee, J.; Hirao, A.; Nakahama, S. *Macromolecules* **1998**, *21*, 274−276.

(14) Zalusky, A. S.; Olayo-Valles, R.; Taylor, C. J.; Hillmyer, M. A. *J. Am. Chem. Soc.* **2001**, *123*, 1519−1520.

(15) Zalusky, A. S.; Olayo-Valles, R.; Wolf, J. H.; Hillmyer, M. A. *J. Am. Chem. Soc.* **2002**, *124*, 12761−12773.

(16) Chen, L.; Phillp, W. A.; Cussler, E. L.; Hillmyer, M. A. *J. Am. Chem. Soc.* **2007**, *129*, 13786−13787.

(17) Chen, L.; Hillmyer, M. A. *Macromolecules* **2009**, *42*, 4237−4243.

(18) Wolf, J. H.; Hillmyer, M. A. *Langmuir* **2003**, *19*, 6553−6560.

(19) Pitet, L. M.; Amendt, M. A.; Hillmyer, M. A. *J. Am. Chem. Soc.* **2010**, *132*, 8230−8231.

(20) Rzayev, J.; Hillmyer, M. A. *J. Am. Chem. Soc.* **2005**, *127*, 13373−13379.

(21) Guo, F.; Jankova, K.; Schulte, L.; Vigild, M. E.; Ndoni, S. *Macromolecules* **2008**, *41*, 1486−1493.

(22) Bailey, T. S.; Rzayev, J.; Hillmyer, M. A. *Macromolecules* **2006**, *39*, 8772−8781.

(23) Guo, F.; Jankova, K.; Schulte, L.; Vigild, M. E.; Ndoni, S. *Langmuir* **2010**, *26*, 2008−2013.

(24) Mao, H.; Arrechea, P. L.; Bailey, T. S.; Johnson, B. J. S.; Hillmyer, M. A. *Faraday Discuss* **2005**, *128*, 149−162.

(25) Yang, S. Y.; Son, S.; Jang, S.; Kim, W. J.; Kim, J. K. *Nano Lett.* **2011**, *11*, 1032−1035.
(26) Misner, M. J.; Skaff, H.; Emrick, T.; Russell, T. P. *Adv. Mater.* **2003**, *15*, 221−224.
(27) Liu, G.; Ding, J.; Stewart, S. *Angew. Chem., Int. Ed.* **1998**, *38*, 835−838.
(28) Drockenmuller, E.; Ll, L. Y. T.; Ryu, D. Y.; Harth, E.; Russell, T. P.; Kim, H. −C.; Hawker, C. J. *J. Polym. Sci., Part A: Polym. Chem.* **2005**, *43*, 1028−1037.
(29) Leiston-Belanger, J. M.; Russell, T. P.; Drockenmuller, E.; Hawker, C. J. *Macromolecules* **2005**, *38*, 7676−7683.
(30) Jeong, U.; Ryu, D. Y.; Kim, J. K.; Kim, D. H.; Wu, X.; Russell, T. P. *Macromolecules* **2003**, *36*, 10126−10129.
(31) Cavicchi, K. A.; Zalusky, A. S.; Hillmyer, M. A.; Lodge, T. P. *Macromol. Rapid Commun.* **2004**, *25*, 704−709.
(32) Guo, F.; Andreasen, J. W.; Vigild, M. E.; Ndoni, S. *Macromolecules* **2007**, *40*, 3669−3675.
(33) Zhou, N.; Bates, F. S.; Lodge, T. P. *Nano Lett.* **2006**, *6*, 2354−2357.
(34) Okumura, A.; Nishikawa, Y.; Hashimoto, T. *Polymer* **2006**, *47*, 7805−7812.
(35) Seo, M.; Amendt, M. A.; Hillmyer, M. A. *Macromolecules* **2011**, *44*, 9310−9318.
(36) Uehara, H.; Yoshida, T.; Kakiage, M.; Yamanobe, T.; Komoto, T.; Nomura, K.; Nakajima, K.; Matsuda, M. *Macromolecules* **2006**, *39*, 3971−3974.
(37) Han, S.; Hagiwara, M.; Ishizone, T. *Macromolecules* **2003**, *36*, 8312−8316.
(38) Gordon, M.; Taylor, J. S. *J. Appl. Chem.* **1952**, *2*, 493−500.
(39) Ji, H.; Sato, N.; Nonidez, W. K.; Mays, J. W. *Polymer* **2002**, *43*, 7119−7123.
(40) Matyjaszewski, K.; Shipp, D. A.; Wang, J.-L.; Grimaud, T.; Patten, T. E. *Macromolecules* **1998**, *31*, 6836−6840.
(41) Shipp, D. A.; Wang, J.-L.; Matyjaszewski, K. *Macromolecules* **1998**, *31*, 8005−8008.
(42) Bielawski, C. W.; Morita, T.; Grubbs, R. H. *Macromolecules* **2000**, *33*, 678−680.
(43) Hahn, S. F. *J. Polym. Sci., Part A: Polym. Chem* **1992**, *30*, 397−408.
(44) Cser, F. *J. Appl. Polym. Sci.* **2001**, *80*, 2300−2308.
(45) Myers, S. B.; Resister, R. A. *Macromolecules* **2010**, *43*, 393−401.
(46) Aggarwal, S. L.; Sweeting, O. J. *Chem. Rev.* **1957**, *57*, 665−742.
(47) Witzke, D. R.; Kolstad, J. J.; Narayan, R. *Macromolecules* **1997**, *30*, 7075−7085.
(48) Wunderlich, W. In *Polymer Handbook*, 4th ed.; Brandrup, J.; Immergut, E. H.; Grulke, E. A., Eds.; Wiley: New York, 1999; p V/87.
(49) Brunauer, S.; Deming, L. S.; Deming, W. E.; Teller, E. *J. Am. Chem. Soc.* **1940**, *62*, 1723−1732.
(50) Barret, E. P.; Joyner, L. G.; Halenda, P. P. *J. Am. Chem. Soc.* **1951**, *73*, 373−380.